ANDREW R. MCCLUSKEY

for the degree of DOCTOR OF PHILOSOPHY

COARSE-GRAINED MODELLING FOR SOFT MATTER SCATTERING

UNIVERSITY OF BATH
DEPARTMENT OF CHEMISTRY

DIAMOND LIGHT SOURCE

Copyright © 2019 Andrew R. McCluskey

Attention is drawn to the fact that copyright of this thesis rests with the author. A copy of this thesis has been supplied on condition that anyone who consults it is understood to recognise that its copyright rests with the author and that they must not copy it or use material from it except as permitted by law or with the consent of the author.

This work is licensed under a Creative Commons "Attribution 4.0 International" license.

First printing, April 2019

“ATTICUS TOLD ME TO DELETE THE ADJECTIVES AND I’D HAVE THE FACTS.”

Scout Finch – To Kill a Mockingbird

Declaration of Authorship

I, Andrew R. McCluskey, declare that this thesis titled "Coarse-grained modelling for soft matter scattering" and the work presented in it are my own. I confirm that:

- where the thesis or any part of the thesis such as a published paper, has been produced jointly with others, that a substantial part is the original work of myself, and
- where the thesis incorporates material already submitted for another degree, the extent of that material and the degree, if any, obtained.

Signed:

Date:

Publications

Some of the information in Chapter 2 has been previously published in:

- A. R. McCluskey et al. *Curr. Org. Chem.* 22.8 (2018), pp. 750–757.

Some of the work covered in Chapter **??** has been previously published in:

- A. R. McCluskey et al. *Phys. Chem. Chem. Phys.* 21.11 (2019), pp. 6133–6141.

Some of the work covered in Chapter **??** has been previously published in:

- A. R. McCluskey et al. *J. Phys. Comm.* Accepted (2019).

Some of the work covered in Chapter **??** has been previously published in:

- A. R. McCluskey et al. *J. Open Source Educ.* 1.2 (2018), pp. 19–21.
- A. R. McCluskey et al. *J. Appl. Crystallogr.* Accepted (2019).

Reproducibility Statement

This thesis exists as a piece of completely reproducible research. I have endevoured to include as much algorithmic and methodological detail within the text, and where relevant working Code Blocks written in Python, and including appropriate documentation strings in the NumPy format, have been included for clarity.

However, in order to provide complete, and easy, reproducibility an electronic supplementary information (ESI) is available online in the form of a Git repository. This ESI provides full details of the analyses performed in this work and access to an automated analysis workflow.

The ESI may be accessed at the following doi:10.5281/zenodo.xxxxxxx.

Acknowledgements

This is where I will acknowledge people. Need to remember everyone...

Contents

List of Figures

List of Tables

List of Abbreviations

ACMW	air-contrast matched water
APM	area per molecule
cmc	critical micelle concentration
$C_{10}TA^+$	*n*-decyltrimethylammonium
$C_{16}TAB$	*n*-hexadecyltrimethylammonium bromide
CCP-SAS	collaborative computational project for small angle scattering
CPU	central processing unit
DDM	*n*-dodecyl-β-*D*-maltoside
DE	differential evolution
DES	deep eutectic solvent
DLS	Diamond Light Source
DM	*n*-decyl-β-*D*-maltoside
DMSO	dimethyl sulfoxide
DLPC	1,2-dilauroyl-*sn*-glycero-3-phosphocholine
DMPC	1,2-dimyristoyl-*sn*-glycero-3-phosphocholine
DMPG	1,2-dimyristoyl-*sn*-glycero-3-phospho-(1'-rac-glycerol)
DCPC	1,2-distearoyl-*sn*-glycero-3-phosphocholine
DPPC	1,2-dipalmitoyl-*sn*-glycero-3-phosphocholine
DPC	dodecylphosphocholine
DPD	dissipative particle dynamics
DVTD	differential vibrating tube densimetry
ESI	electronic supplementary information
ESRF	European Synchrotron Radiation Facility
ESS	European Spallation Source
GIXD	grazing-incidence X-ray diffraction
GPU	graphical processing units
hdDES	partially deuterated deep eutectic solvent
hDES	hydrogenated deep eutectic solvent
ILL	Institut Laue-Langevin
LC	Liquid-Condensed
LE	Liquid-Expanded
MCMC	Markov chain Monte Carlo
MD	molecular dynamics
MPI	message passing interface
NB	neutral buoyancy
NPT	constant number, pressure, and temperature
NR	neutron reflectometry

NVE	constant number, volume, and energy
NVT	constant number, volume, and temperature
OER	open education resource
PC	phosphocholine
PDF	probability distribution function
PFTE	polytetrafluoroethylene
PG	phosphatidylglycerol
PME	particle mesh Ewald
PSO	particle swarm optimisation
RDF	radial distribution function
SANS	small angle neutron scattering
SAS	small angle scattering
SDS	sodium dodecyl sulfate
SLD	scattering length density
SAXS	small angle X-ray scattering
SPC	single point charge
STFC	Science & Technology Facilities Council
ToF	time-of-flight
VMD	visual molecular dynamics
wph	water molecules per head group
WAXS	wide angle X-ray scattering
XRR	X-ray reflectometry

Physical Constants

	$\pi = 3.1415\ldots$
Planck constant	$h = 6.626\ \ldots \times 10^{-34}\,\mathrm{J\,s}$
Golden ratio	$\Phi = 1.618\ \ldots$
dielectric permittivity of the vacuum	$\epsilon_0 = 8.854\ \ldots \times 10^{-12}\,\mathrm{F\,m^{-1}}$
charge of electron	$e = 1.602\ \ldots \times 10^{-19}\,\mathrm{C}$
Boltzmann constant	$k_B = 1.381\ \ldots \times 10^{-23}\,\mathrm{J\,K^{-1}}$

List of Symbols

a	step size	
a_0	optimum head-group area	m^2
b	scattering length	m
b	bond length	m
b_i	best candidate solution	
b_0	equilibrium bond length	m
d_h	phosphlipid head layer thickness	m
d_t	phosphlipid tail layer thickness	m
d_x	length of object	m
k_m	mutation constant	
l_0	length of hydrophobic tail	m
m	mass	kg
n	number of scattering vectors	
n_i	refractive index	
p	packing parameter	
p	parallel component	
q	scattering magnitude	m^{-1}
$q_{i,j}$	electronic charge	
r	displacement vector magnitude	m^{-1}
$r_{n,n+1}$	Fresnel equation coefficient	
s	serial component	
t	time	s
t_F	time-of-flight	s
$A_{1,2,3}$	dihedral constants	J
B	resultant matrix	
E_{bonded}	bonded energy	J
E_k	kinetic energy	J
$E_{\text{non-bonded}}$	non-bonded energy	J
E_{total}	total energy	J
F	some function	
I	intensity	
K_b	bond force constant	$\mathrm{J\,m}^{-2}$
K_θ	angle force constant	$\mathrm{J\,rad}^{-2}$
L_F	length-of-flight	m
M_n	layer matrix	
N	number of some item	
N_P	number of magnets	

N_ρ	number density	
$P(q)$	form factor	
R	reflected intensity	
$R1, 2$	some random number	
R_g	radius of gyration	m
R_i	incidence rate	s^{-1}
R_s	radius of sphere	m
S	surface area	m^2
$S(q)$	structure factor	
T	temperature	K
U	uniform distribution	
V	volume	m^3
V_c	volume of hydrophobic tail	m^3
V_h	phosphlipid head volume	m^3
V_n	volume of layer	m^3
V_p	volume of particle	m^3
V_t	phosphlipid tail volume	m^3
$\mathbf{a}$	acceleration	$\mathrm{m\,s}^{-2}$
$\mathbf{f}$	force	N
$\mathbf{g}$	global best	
$\mathbf{k}_i$	incident wavevector	m^{-1}
$\mathbf{k}_f$	final wavevector	m^{-1}
$\mathbf{m}$	mutant vector	
$\mathbf{o}$	offspring population	
$\mathbf{p}$	parent population	
$\mathbf{q}$	scattering wavevector	m^{-1}
$\mathbf{r}$	displacement	m
$\mathbf{s}$	personal best	
$\mathbf{v}$	velocity	$\mathrm{m\,s}^{-1}$
$\mathbf{x}$	position	m
$\mathbf{R}$	particle position	m
β_c	fraction of the speed of light	
β_n	phase factor	
δ	infinitesimally small change	
ε	depth of potential well	J
ζ	figure of merit	
2θ	scattering angle	rad
θ	angle	rad
θ	some solution	
θ_0	equilibrium angle	rad
θ_c	critical angle	rad
θ_e	angle between electron and photon	rad
λ	wavelength	m
π	surface pressure	$\mathrm{mN\,m}^{-1}$
σ	distance at zero	m
σ_{coh}	coherent scattering cross-section	m
σ_{incoh}	incoherent scattering cross-section	m
$\sigma_{n,n+1}$	interfacial roughness	m

ϕ	scattering angle	
ϕ	dihedral angle	rad
ϕ_g	global acceleration coefficient	
ϕ_i	volume fraction of solvation	
ϕ_p	personal acceleration coefficient	
χ^2	a figure of merit	
ψ_0	wave at point 0	
ψ_i	wave at point i	
ψ_f	final scattered wave	
ω	frequency	s^{-1}
ω	initial weight	
ω_i	incident frequency	s^{-1}
ω_f	final frequency	s^{-1}
Δt	timestep	s
Θ	new solution	
Φ	incident flux	
$\mathrm{d}\sigma(q)/\mathrm{d}\Omega$	differential cross-section	

Abstract

This work uses different coarse-graining methodologies to assist in the analysis of scattering measurements from soft matter species, such as surfactant monolayers and micelles. The term 'coarse-graining' is used broadly in this work; to describe the coarse-graining of a classical simulation potential model, a surfactant monolayer model that consists two layers, and a severe coarse-graining methodology that describes a surfactant molecule as just a position and direction in space. In all three cases, the aim of the applied coarse-graining is to improve the methods of analysis that may be performed in the analysis of reflectometry and small angle scattering measurements.

A surfactant monolayer model, that was considerate of the chemical bond between the surfactant heads and tails, was developed for the analysis of reflectometry measurements from a phospholipid monolayer at the interface between air and a deep eutectic solvent. This model allowed for a unique insight into the structure of the monolayer at the given interface. To assess the utility of coarse-grained potential modesl in the analysis of neutron reflectometry, a phospholipid monolayer was simulated using three different potential models, of different particle grain-size. This allowed for a better undertstanding of the simulation resolution necessary to accurately and successfully apply simulation-driven analysis to reflectometry. Finally, a severely coarse-grained description of a surfactant was used in a particle swarm optimisation to try and develop a starting structure for a multiple micelle simulation, where the experimental scattering profile was the optimisation target.

Alongside the development and application of coarse-graining methodologies, the final chapter of this work describes the development of open-source software and teaching materials for the introduction of classical molecular simulation. These educational resources introduce scattering users to simulation and its utility in scattering analysis, to enable a future where simulation driven analysis may be performed accurately by all.

1

Introduction

Soft matter is an umbrella term for many different types of material. These include micelles; sub-micron sized, dynamic agglomerates of amphiphilic molecules such as surfactants or block copolymers, colloidal solutions; where the interaction between the colloids may be controlled through chemical modification, or proteins; where the polar nature of different amino acids leads to the protein folding into a highly organised, and biologically relevant, shape. Some examples of these soft matter systems are shown in Figure 1.1. These species, initially, appear rather disparate, however, there are a few important commonalities among soft matter systems:[1]

- the lengths scales are intermediate between atomistic and macroscopic,[2]
- for soft matter systems the energy of a structural distortion is similar to thermal energy, so the material is in constant flux,
- this thermal motion can lead to the formation of complex, hierarchical structures due to the balance between enthalpy and entropy, this process is refered to as self-assembly.

[1] R. A. L. Jones. *Soft Condensed Matter*. 2002.

[2] typically 1×10^{-8}-1×10^{-5} m.

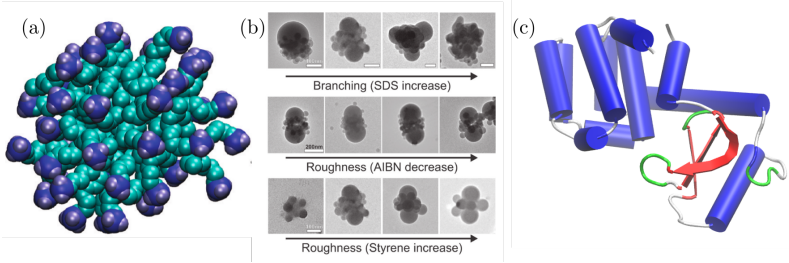

Figure 1.1: Three examples of soft matter species; (a) a 43 C_{10}TAB surfactant micelle, reprinted with permission from R. Hargreaves et al. *J. Am. Chem. Soc.* 133.41 (2011), pp. 16524–16536, copyright 2011 American Chemical Society, (b) the tunable interactions of colloids, reprinted with permission from D. J. Kraft et al. *J. Phys. Chem. B* 115.22 (2011), pp. 7175–7181, copyright 2011 American Chemical Society, and (c) generated using VMD (W. Humphrey et al. *J. Mol. Graph.* 14.1 (1996), pp. 33–38) from the crystal structure of T4-lysozyme D. R. Rose et al. *Protein Eng. Des. Sel.* 2.4 (1988), pp. 277–282.

1.1 Soft matter self-assembly

Soft matter self-assembly is the ability for soft matter systems to form organised structures in solution. These are of particular interest industrially, where surfactant and polymer self-assembly play

an import role in food, commodity, and speciality chemicals.[3] Self-assembly processes are important from a biological perspective as it is phospholipids, a family of surface-active biomolecules, which make up the bilayers that protect cells.[4] The structures that result from the self-assembly of soft matter species have fluid-like properties. This is due to the fact that the subunits are held together by weak forces such as the van der Waals, hydrophobic, hydrogen-bonding, and screen electrostatic interactions.[5] This means that the structure of a self-assembled species is susceptible to changes in the local chemical environment, such as pH or salt concentration.[6]

The focus of this work is on the self-assembly of surfactant molecules. Surfactant is a general term for any molecule which is "surface-active", to say that they will interact at an interface.[7] Surfactants are generally made up of two components; one part is highly soluble in one of the interfacial phases, while the other is not.[8] Usually, surfactants consist of a hydrocarbon tail, which is hydrophobic, and some hydrophilic head group, which can be ionic or non-ionic. When surfactants are present in water, the two components will interact differently with the solvent. A hydration sphere of water molecules will form around the hydrophilic head group, effectively allowing the head group to take part in the water's hydrogen-bonding network. Whereas, the lyophilic tail has a structure-breaking effect on the hydrogen bonding network, termed the "hydrophobic effect". The free energy deficit of this structure-breaking can be reduced through the aggregation of these hydrophobic groups, as the van der Waals attraction between tail groups is larger than that present between tail groups and water molecules. There is a decrease in entropy from the tail organisation, however, this is offset by the entropic increase from the water structure breakup. Finally, by considering the effect of the, often charged, head groups being close together, it is thought that the majority of the charge can be screened by the presence of a counter-ion, or water molecules, bound to the head group.[9] This means that at low concentrations, where it is statistically unlikely for an agglomerate to form, the majority of surfactants will sit at the air-water interface, as the concentration is increased, assuming the system is above the Krafft temperature,[10] organised structures wil begin to appear.

The structures can be formed from surfactant solutions are diverse; featuring micellar, hexagonal, cubic, and lamallar mesophases. These mesophases have a significant impact on the macroscopic properties of the system, for example the liquid crystalline hexagonal phase can present interesting viscoelastic behaviour.[11] The mesophase that is formed is dependent on the shape of the underlying surfactants, Israelachvili described this dependency in terms of the dimensionless surfactant packing parameter, p.[12]

$$p = \frac{V_c}{a_0 l_0}, \tag{1.1}$$

[3] L. L. Schramm et al. *Annu. Rep. Prog. Chem., Sect. C: Phys. Chem.* 99 (2003), pp. 3–48.

[4] K. Simons et al. *Nat. Rev. Mol. Cell Biol.* 1 (2000), pp. 31–39.

[5] J. Israelachvili. *Intermolecular and Surface Forces*. 2011.

[6] D. Schmaljohann. *Adv. Drug Deliv. Rev.* 58.15 (2006), pp. 1655–1670; M. Sammalkorpi et al. *J. Phys. Chem. B* 113.17 (2009), pp. 5863–5870.

[7] M. J. Rosen et al. *Surfactants and Interfacial Phenomena*. 2012.

[8] J. Goodwin. *Colloids and Interfaces with Surfactants and Polymers*. 2009.

[9] Goodwin, see n. 8.

[10] The lowest temperature at which agglomerates will form.

[11] D. Jurašin et al. *Soft Matter* 9.12 (2013), p. 3349; F. Cordobés et al. *J. Colloid Interface Sci.* 187.2 (1997), pp. 401–417.

[12] Israelachvili, see n. 5.

where, V_c is the volume of the hydrophobic tail, l_0 is the length of the tail, and a_0 is the optimum head group area. This parameter can be used to estimate the geometry of the resulting self-assembled structure, detailed in Figure 1.2. It is important to note that the optimum head group area accounts for the hydration sphere of the head group. A short tail surfactant, such as *n*-decyltrimethylammounium bromide,[13] will have a very small packing parameter resulting in small spherical micelles. Whereas, the twin-tailed phospholipids, such as 1,2-dipalmitoyl-*sn*-glycero-3-phosphocholine,[14], will have a much larger packing parameter due to the larger tail volume and length, therefore this surfactant will for, a lamellar bilayer in solution.

[13] Commonly abbreviated to C_{10}TAB.

[14] Known as DPPC.

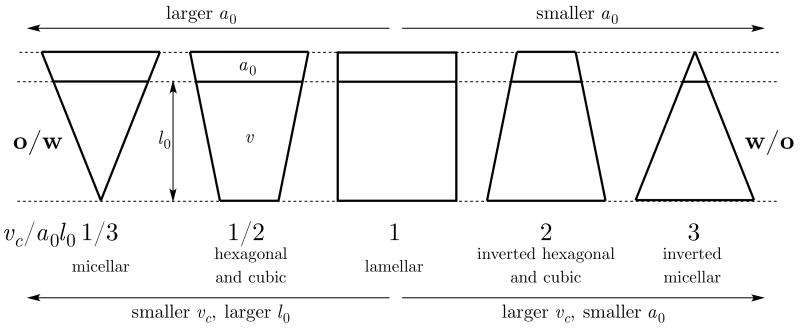

Figure 1.2: A graphical representation of the packing parameters and information of the resulting self-assembled structure.

This work will focus on the investigation of surfactant monolayers and micellar systems. These represent interesting model systems of significant interest both technologically[15] and biologically.[16] Both of these systems are regularly investigated using X-ray and neutron elastic scattering techniques, with analysis performed in a model-dependent fashion.[17]

[15] N. Anton et al. *Int. J. Pharm.* 398.1-2 (2010), pp. 204–209; M. Zagnoni. *Lab on a Chip* 12.6 (2012), p. 1026.

[16] K. Kataoka et al. *Adv. Drug Deliv. Rev.* 64 (2012), pp. 37–48; H Mohwald. *Annu. Rev. Phys. Chem.* 41 (1990), pp. 441–476; S. Kewalramani et al. *J. Phys. Chem. Lett.* 1.2 (2010), pp. 489–495.

[17] E. Pambou et al. *Langmuir* 31.36 (2015), pp. 9781–9789; D. W. Hayward et al. *Macromolecules* 48.5 (2015), pp. 1579–1591; I. Rodriguez-Loureiro et al. *Soft Matter* 13.34 (2017), pp. 5767–5777; G. Hazell et al. *J. Colloid Interface Sci.* 474 (2016), pp. 190–198.

1.2 Analysis of soft matter scattering

The use of neutron and X-ray scattering experiments for the study of soft matter is well developed, with early research into the structure of phospholipid monolayers by reflectometry methods being conducted in the late 1970s by Albrecht *et al.*[18] While, the work of Kratky and Porod,[19] who used small angle X-ray scattering for the study of colloidal systems was published in 1949. Since these early works, instrumentation developments have enabled more challenging experiments to be conducted, such as time-resolved studies[20] and the study of floating lipid bilayers.[21]

However, the analysis of soft matter scattering has changed little since these early works, still typically involving the use of very coarse models. These include the shape-based modelling common in small angle scattering[22] and reflectometry analysis.[23] More sophisticated model refinements have been developed, such as the use of Monte-Carlo sampling,,[24] differential evolution opti-

[18] O. Albrecht et al. *J. Phys. France* 39.3 (1978), pp. 301–313.

[19] O Kratky et al. *J. Colloid Sci.* 4.1 (1949), pp. 35–70.

[20] G. V. Jensen et al. *Angew. Chemie Int. Ed.* 53.43 (2014), pp. 11524–11528.

[21] V. Rondelli et al. *J. Phys. Conf. Ser.* 340 (2012), p. 012083.

[22] P. A. Hassan et al. *J. Colloid Interface Sci.* 257.1 (2003), pp. 154–162, see Section **??**.

[23] R. A. Campbell et al. *J. Colloid Interface Sci.* 531 (2018), pp. 98–108; J. R. Lu et al. *Acta Crystallogr. A* 52.1 (1996), pp. 11–41, see Section **??**.

[24] J. S. Pedersen. "Monte Carlo Simulation Techniques Applied in the Analysis of Small-Angle Scattering Data from Colloids and Polymer System". In: *Neutron, X-Rays and Light. Scattering*

misation,[25] and Bayesian inference.[26] However, there has been little change in the definition of the models that unpin the analysis processes. Recently, there have been movements towards the use of atomistic modelling techniques[27] to augment, and assist, the analysis of soft matter scattering measurements, in a multi-modal approach.[28]

Much of the work relating to the use of atomistic simulation for the analysis of small angle scattering measurements has been focused on the study of protein molecules in solution.[29] This has allowed for a more profound understanding aspects of biology suhc as the conformational states available to protein molecules in solution.[30] The uptake of atomistic simulation for the analysis of small angle scattering from systems such as micelles has been slower, in part due to the more complex conformation landscape available to these systems under standard conditions. However, the work of Hargreaves *et al.* paired atomistic simulation with total scattering measurements[31] to resolve the structure of an simple short-tail surfactant micelle.[32] Further, the work of Ivanović *et al.* used scattering experiments to refine the output of molecular dynamics simulations of micelles of a pre-defined size.[33] Both of these examples required significant computational resource; in the former case, the computational time taken was quoted as 200 days, while the later required the running of multiple simulations at different micelle sizes in order to determine the appropriate simulation.

The use of atomistic simulation for the analysis reflectometry measurements of soft matter systems began with the work of Miller *et al.* and Anderson and Wilson,[34] where atomistic simulations[35] were used to study polymer self-assembly at the oil-water interface. These simulation trajectories was then compared with experimental neutron reflectometry measurements. Dabkowska *et al.* also used atomistic simulation and neutron reflectometry measurements to study the structure of a surfactant monolayer at the air-water interface, providing the first example of a direct comparison between experimental reflectometry data and that determined from simulation.[36] To date, there is only one work that has used coarse-grained molecular dynamics simulation to aid in the analysis of neutron reflectometry, this is the work of Koutsioubas.[37] This work made use of the MARTINI coarse-grained forcefield to simulate a lipid bilayer, and was compared with experimental neutron reflectometry measurements.

1.3 Coarse-graining of soft matter systems

The characteristic non-atomistic length scales associated with soft matter systems make them ideal for the application of coarse-graining protocols. Coarse-graining is where dimensionality of a problem is reduced by the removal of certain degrees of freedom

[25] M. Wormington et al. *Philos. Trans. R. Soc. London Ser. A* 357.1761 (1999), pp. 2827–2848.

[26] A. R. J. Nelson et al. *J. Appl. Crystallogr.* 52.1 (2019), pp. 193–200.

[27] Such as molecular dynamics.

[28] E. Scoppola et al. *Curr. Opin. Colloid Interface Sci.* 37 (2018), pp. 88–100.

[29] The historical context of this is discussed briefly in Chapter **??**.

[30] S. Bowerman et al. *J. Chem. Theory Comput.* 13.6 (2017), pp. 2418–2429.

[31] In the form of Emperical Potential Structure Refinement.

[32] R. Hargreaves et al. *J. Am. Chem. Soc.* 133.41 (2011), pp. 16524–16536.

[33] M. T. Ivanović et al. *Angew. Chemie Int. Ed.* 57.20 (2018), pp. 5635–5639.

[34] A. F. Miller et al. *Mol. Phys.* 101.8 (2003), pp. 1131–1138; P. M. Anderson et al. *J. Chem. Phys.* 121.17 (2004), p. 8503.

[35] Monte Carlo and molecular dynamics respectively.

[36] A. P. Dabkowska et al. *Langmuir* 30.29 (2014), pp. 8803–8811.

[37] A. Koutsioubas. *J. Phys. Chem. B* 120.44 (2016), pp. 11474–11483.

from a set. The most common method of coarse-graining is the re-parameterisation of an atomistic molecular dynamics potential model in terms of this reduced parameter space. An example of this is the MARTINI forcefield,[38] where the aim is to reparameterise the system without significant loss of chemical information.[39] A result of coarse-graining is the creation a flatter potential energy landscape, as shown in Figure 1.3. However, in this work I have also investigated the effect of applying a chemically-consistent coarse-grained monolayer model for the analysis of reflectometry data,[40] This system is coarse-grained so as to describe a phospholipid material as consisting of a head group and pair of tail groups. Additionally, I have assessed the efficacy of different atomistic and coarse-grained potential models for the analysis of neutron reflectometry, building on the work of Dabkowska *et al.* and Koutsioubas.[41]

[38] This specific model is discussed in greater detail in Section **??**.

[39] S. J. Marrink et al. *J. Phys. Chem. B* 111.27 (2007), pp. 7812–7824.

[40] This work is the focus of Chapter **??**.

[41] Dabkowska et al., see n. 36; Koutsioubas, see n. 37, see Chapter **??**.

1.4 Optimisation methodologies

The availability of high performance computing has increased significantly in recent years, in particular due to cloud-based infrastructures. Furthermore, highly parallelisable optimisation algorithms are now available such as the particle swarm[42] and differential evolution[43] optimisations. As mentioned above, previous work has shown that the simulation of a surfactant micelle and comparison with experimental data requires significant computational expense[44] In the interest of reducing this, and improving the applicibility of high performance computing to simulation-driven analysis of small angle scattering I have investigated the use of a particle swarm optimisation (PSO) to produce a realistic, near-atomistic micelle structure based on experimental data alone. This has made use of a coarse-grained description of a surfactant molecule on two levels; one for the particle swarm optimisation and another for the scattering profile calculation.[45].

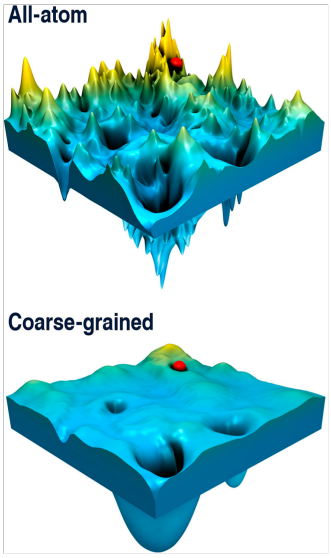

Figure 1.3: Potential energy surfaces for an all-atom vs a coarse-grained potential model, reprinted with permission of the American Chemical Society from S. Kmiecik et al. *Chem. Rev.* 116.14 (2016), pp. 7898–7936.

[42] J. Kennedy et al. In: *Proceedings of ICNN'95*. International Conference on Neural Networks. Perth, AU, 1995, pp. 1942–1948; Y. Shi et al. In: *1998 IEEE International Conference on Evolutionary Computation Proceedings*. IEEE World Congress on Computational Intelligence. Anchorage, US, 1998, pp. 69–73.

[43] R. Storn et al. *J. Global Optim.* 11 (1997), pp. 341–359.

[44] Hargreaves et al., see n. 32; Ivanović et al., see n. 33.

[45] See Chapter **??**.

1.5 Educational materials

While the development of analytical methods and infrastructure are important for the development and uptake of the simulation-driven analysis methods applied in this work, the development of informatative resources is also necessary. Current experimental users of small angle scattering are typically not familiar with detailed aspects of classical simulation, however, they are often interested in applying it to assist with their analyses. Therefore, alongside traditional research applications, I have been developing open educational resources[46] designed to introduce classical simulation techniques, and to allow users of scattering techniques to become familiar with these. The ambition being that as the availablility of simulation-driven analysis for small angle scattering

[46] Abbreviated to OERs

grows, so will the user base that is familiar with the underlying methods.[47]

[47] See Chapter **??**.

2
Theory

2.1 Probing radiation

This work is focussed on the use of X-ray and neutron scattering to probe soft matter systems; in particular surfactant monolayers and micelles. Therefore, it is pertinent to discuss how each of these probing radiation is produced and detail the advantages of each with respect to the other.

2.1.1 Generation of X-rays

X-rays are a form of electromagnetic radiation similar to visible light, albeit with a much shorter wavelength.[1] There are four common ways to produce X-rays; three are available within the laboratory, while the other is exclusive to large scale facilities.

The three laboratory source X-ray generation techniques are the X-ray tube, the rotating anode, and the liquid jet. An X-ray tube consists of a filament and an anode within a vacuum chamber, by passing a high voltage electrical current across the filament electrons are emitted which accelerate towards the anode. On collision with the anode, the rapid deceleration results in the emission of X-rays at a characteristic wavelength based on the anode material.[2] The most common material for an X-ray tube anode is copper which gives off radiation with an energy of $\sim 8\,\mathrm{keV}$.[3]

Another common laboratory method for the generation of X-rays is the rotating anode.[4] In the X-ray tube, each time that an electron collides with anode there is some energy transfer, this means that over many millions of collisions the temperature of the anode can rise significantly, which can cause the anode material to melt. Resulting in a temperature-based limitation to the available X-ray flux. This lead to the development of the rotating anode, which is simply where the anode is made from a rotating wheel, such that the bombardment is spread across the whole wheel reducing the energy localisation. The use of a rotating anode can allow for an increase in the photon flux by about an order of magnitude.[5]

The final laboratory method for X-ray generation is the liquid jet source.[6] For the liquid jet X-ray source, an electron beam is

[1] Typically $0.01\text{-}10\,\mathrm{nm}$.

[2] H. Schnablegger et al. *The SAXS Guide: Getting Acquainted with the Principles*. 2017.

[3] This is a wavelength of $\sim 1.5\,\mathrm{nm}$.

[4] Essentially an improvement on the X-ray tube.

[5] Schnablegger et al., see n. 2.

[6] *MetalJet X-Ray Source Technology*. URL: https://www.excillum.com/technology/ (Accessed 2018-12-6), Branded MetalJet by excillum.

incident on a liquid metal sample,[7] rather than traditional solid metal, which can dissipate heat more efficiently. This means that the electron intensity and therefore X-ray brightness, available to the liquid jet source is much greater than a rotating anode source.

[7] Usually an gallium or indium alloy.

The method of X-ray generation that is not available in a typical laboratory is at a synchrotron, the use of this method has the drawback that it requires access to a national or international facility.[8] The way in which X-rays are generated at a synchrotron involves the acceleration of an electron, rather than the deceleration as with the laboratory sources. This is achieved by having relativistic electrons travel on a curve, from Newtonian mechanics it is known that travelling on a curve at constant speed is equivalent to acceleration. First the electrons are accelerated, after being produced in a linear accelerator, to near the speed of light in a booster synchrotron before injecting them into the storage ring. In the storage ring, the electrons are kept at relativistic speeds with bending magnets and straight sections making up a ring as shown in Figure 2.1. How circular the ring is depends on the number of bending magnets that make it up; for example, DLS had 48 bending magnets with 48 straight sections at the time of construction.

[8] Such as Diamond Light Source (DLS) or the European Synchrotron Radiation Facility (ESRF).

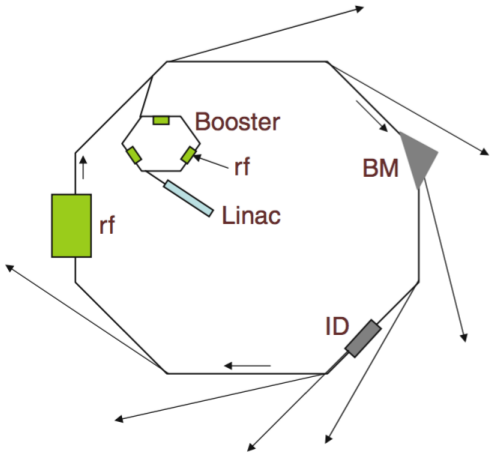

Figure 2.1: A schematic representation of a synchrotron radiation source, identifying the Linac, the booster ring, the radio-frequency cavities (rf), the bending magnet (BM) and the insertion device (ID), reprinted by permission of Springer Nature Customer Service Centre GmbH: Springer Nature from M. C. Garcia-Gutierrez et al. "Bases of Synchrotron Radiation, Light Sources, and Features of X-Ray Scattering Beamlines". In: *Applications of Synchrotron Light to Scattering and Diffraction in Materials and Life Sciences*. 2009, pp. 1–22.

When an electron accelerates (or travels on a curve), Cherenkov radiation is emitted in accordance with the Cherenkov relation,

$$n_i \beta_c \cos\theta_e = 1, \tag{2.1}$$

where, n_i is the refractive index for the dielectric medium, β_c is the fraction of the speed of light at which that electron is travelling, and θ_e is the angle between the electron trajectory and the trajectory of the resulting photon.[9] The curve is the result of a bending magnet, meaning that at each bending magnet there can be a beamline which uses the synchrotron light. The light that is given off from a bending magnet is continuous and broad, covering a wide range of the electromagnetic spectrum. The alternative to a bending magnet beamline is that which is served by an insertion device.

[9] M. C. Garcia-Gutierrez et al. "Bases of Synchrotron Radiation, Light Sources, and Features of X-Ray Scattering Beamlines". In: *Applications of Synchrotron Light to Scattering and Diffraction in Materials and Life Sciences*. 2009, pp. 1–22.

An insertion device is able to offer more specific radiation characteristics (photon energy, narrower band) than a bending magnet, and are placed on the straight sections of the synchrotron. Common insertion devices include wavelength shifters, wigglers, and undulators.

The type of insertion device that is present at both I07 and I22 at DLS is an undulator. An undulator consists of a series of magnets of opposing polarity that causes the electrons to 'wiggle' back and forth as shown in Figure 2.2. This results in a superposition of radiation from N_P sources, where N_P is the number of magnets, yielding quasi-monochromatic radiation. The brilliance of different X-ray sources are compared in Table 2.1, this shows the significant benefit that an undulator can offer in terms of photon brilliance.

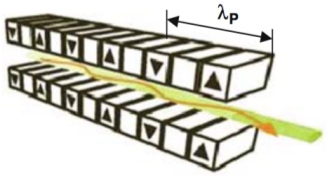

Figure 2.2: A diagram of an undulator insertion device, such as that on I07 and I22, where λ_P is the period length between opposing magnets, reprinted by permission of Springer Nature Customer Service Centre GmbH: Springer Nature from Garcia-Gutierrez et al., "Bases of Synchrotron Radiation, Light Sources, and Features of X-Ray Scattering Beamlines".

[10] This is discussed in detail in Section **??**.

2.1.2 Generation of neutrons

Neutrons hold an advantage over X-rays, particularly for application to the study of soft matter, due to the ability to use contrast variation to increase the quantity of information from the sample.[10] However, neutrons cannot be produced safely on a laboratory scale, therefore it is always necessary to visit large scale facilities to harness neutrons for scattering experiments. These facilities come in two flavours; the reactor source and the spallation source, each offering unique benefits.

Neutron reactor sources[11] are currently the most common format of neutron source and are capable of producing the highest average neutron flux.[12] The High-Flux Reactor at the ILL is capable of producing a neutron flux of $1.5 \times 10^{15}\,\text{neutrons}\,\text{s}^{-1}\text{cm}^{-2}$.[13] A reactor source operates on the principle of nuclear fission, where an atomic nucleus is capable of breaking down into smaller nuclei, overcoming the strong nuclear force. This often involves using uranium enriched with its fissile isotope, ^{235}U, which after the initial absorption of a stray neutron[14] will undergo fission to release, on average, 2.5 daughter neutrons, an example of a possible uranium fission mechanism is:

$$\text{n} + {}^{235}\text{U} \longrightarrow {}^{236}\text{U} \longrightarrow {}^{134}\text{Xe} + {}^{100}\text{Sr} + 2\,\text{n}.$$

This type of mechanism is the basis for both research, and nuclear power, reactors.[15] One of the major drawbacks for reactor neutron sources is the perceived public opinion towards such facilities. Major safety concerns, such as "nuclear meltdown" and the resulting

[11] Such as the Institut Laue-Langevin (ILL) in Grenoble, France.

[12] The number of neutrons per second per unit area.

[13] *ILL: Neutron for Science: Technical Characteristics*. URL: https://www.ill.eu/reactor-environment-safety/high-flux-reactor/technical-characteristics/ (Accessed 2016-8-8).

[14] Arising from a cosmic ray, or spontaneous fission.

[15] D. S. Sivia. *Elementary Scattering Theory: For X-Ray and Neutron Users*. 2011.

Light source	Approximate brilliance/ photons $\text{s}^{-1}\text{mrad}^{-2}0.1\%\text{bandwidth}^{-1}$
Candle	1×10^5
X-ray tube	1×10^8
Sun	1×10^{10}
Bending magnet	1×10^{15}
Undulator	1×10^{20}

Table 2.1: A comparision of the photon brilliance from different light sources. Adapted, with permission of Oxford University Press, from D. S. Sivia. *Elementary Scattering Theory: For X-Ray and Neutron Users*. 2011.

nuclear waste, mean that reactor sources are often unpopular and therefore struggle to obtain funding required for operation.

The other form of neutron source is a spallation source, this is much less controversial as it does not require fissile materials and hence there is no risk of a nuclear disaster. The ISIS Neutron and Muon Source is an example of a spallation source, where high energy protons, 800 MeV,[16] are accelerated towards a tungsten target. When the protons strike the target, they can cause the release of a series of neutrons, the first batch of neutrons are given off with too high an energy to be useful, however, less excited neutrons are given off by secondary emissions. In addition to the public perception benefit, spallation sources also offer a technological advantage in the time-of-flight[17] technique. The ToF technique relies the fact that at a spallation source, it is possible to know the time at which the neutron was ejected from the target to a high level of precision and therefore it is possible to measure the time taken for the neutron to reach the instrument. Since the neutron is a particle of a finite mass, m, it is possible to correlate the velocity, $\mathbf{v}$, of the particle with the kinetic energy, E_k,

$$E_k = \frac{m\mathbf{v}^2}{2}, \tag{2.2}$$

and with knowledge of the energy of the particle, its wavelength, λ, can be determined by the de Broglie relation,[18]

$$E = h\omega = \frac{hv}{\lambda}, \tag{2.3}$$

where, h is Planck constant and ω is the neutron frequency. Therefore, the wavelength of the neutron is proportional to the inverse of the particle's velocity, and hence the time-of-flight, t_F,

$$\lambda = \frac{h}{mv} = \frac{ht_F}{mL_F}, \tag{2.4}$$

where, L_F is the distance between the target and the instrument. The fact that the neutrons can spread out in the flight from the target means that wavelength-dispersive techniques, where the neutron wavelength is measured rather than the scattering angle, are possible at spallation sources which cannot be carried out natively at reactor sources. The weakness of current spallation sources is that they have a lower average flux than reactor sources, however, the construction of the European Spallation Source[19] will change this as it offers an average flux similar to that of a reactor source with the benefits of the spallation technique.

A problem that is inherent for both reactor and spallation sources is that the energy of the neutrons given off is usually too high to be used to study condensed materials, such as soft matter. This means that moderation must be used to reduce the energy of the neutrons passing through the sample. The neutrons that are considered to be optimal for the study of condensed materials are

[16] *ISIS – How ISIS Works*. URL: https://www.isis.stfc.ac.uk/Pages/What-does-ISIS-Neutron-Muon-Source-do.aspx (Accessed 2018-9-25).

[17] Abbreviated to ToF.

[18] L. de Broglie. *Ann. Phys. (Paris)* 10.3 (1925), pp. 22–125.

[19] Known as the ESS.

thermal in nature, named because their energy is approximately that of ambient temperature. Thermal neutrons are achieved by allowing the neutrons to pass through a large volume of moderator material, usually, graphite, D_2O, methane or H_2, stored at 300 K before they reach the instrument.[20]

[20] Sivia, see n. 15.

References

Albrecht, O., H. Gruler, and E. Sackmann. "Polymorphism of Phospholipid Monolayers". *J. Phys. France* 39.3 (1978), pp. 301–313. DOI: 10.1051/jphys:01978003903030100.

Anderson, P. M. and M. R. Wilson. "Molecular Dynamics Simulations of Amphiphilic Graft Copolymer Molecules at a Water/Air Interface". *J. Chem. Phys.* 121.17 (2004), p. 8503. DOI: 10.1063/1.1796251.

Anton, N., H. Mojzisova, E. Porcher, J.-P. Benoit, and P. Saulnier. "Reverse Micelle-Loaded Lipid Nano-Emulsions: New Technology for Nano-Encapsulation of Hydrophilic Materials". *Int. J. Pharm.* 398.1-2 (2010), pp. 204–209. DOI: 10.1016/j.ijpharm.2010.07.039.

Bowerman, S., A. S. J. B. Rana, A. Rice, G. H. Pham, E. R. Strieter, and J. Wereszczynski. "Determining Atomistic SAXS Models of Tri-Ubiquitin Chains from Bayesian Analysis of Accelerated Molecular Dynamics Simulations". *J. Chem. Theory Comput.* 13.6 (2017), pp. 2418–2429. DOI: 10.1021/acs.jctc.7b00059.

Campbell, R. A., Y. Saaka, Y. Shao, Y. Gerelli, R. Cubitt, E. Nazaruk, D. Matyszewska, and M. J. Lawrence. "Structure of Surfactant and Phospholipid Monolayers at the Air/Water Interface Modeled from Neutron Reflectivity Data". *J. Colloid Interface Sci.* 531 (2018), pp. 98–108. DOI: 10.1016/j.jcis.2018.07.022.

Cordobés, F., J. Muñoz, and C. Gallegos. "Linear Viscoelasticity of the Direct Hexagonal Liquid Crystalline Phase for a Heptane/Nonionic Surfactant/Water System". *J. Colloid Interface Sci.* 187.2 (1997), pp. 401–417. DOI: 10.1006/jcis.1996.4707.

Dabkowska, A. P., L. E. Collins, D. J. Barlow, R. Barker, S. E. McLain, M. J. Lawrence, and C. D. Lorenz. "Modulation of Dipalmitoylphosphatidylcholine Monolayers by Dimethyl Sulfoxide". *Langmuir* 30.29 (2014), pp. 8803–8811. DOI: 10.1021/la501275h.

De Broglie, L. "Recherches Sur La Théorie Des Quanta". *Ann. Phys. (Paris)* 10.3 (1925), pp. 22–125.

Garcia-Gutierrez, M. C. and D. R. Rueda. "Bases of Synchrotron Radiation, Light Sources, and Features of X-Ray Scattering Beamlines". In: *Applications of Synchrotron Light to Scattering and Diffraction in Materials and Life Sciences*. Ed. by M. Gomez, A. Nogales, M. C. Garcia-Gutierrez, and T. A. Ezquerra. Berlin,

DE: Springer-Verlag Berlin Heidelberg, 2009, pp. 1–22. ISBN: 978-3-540-95968-7.

Goodwin, J. *Colloids and Interfaces with Surfactants and Polymers*. 2nd ed. Chichester, UK: John Wiley & Sons, 2009. ISBN: 978-0-470-51880-9.

Hargreaves, R., D. T. Bowron, and K. Edler. "Atomistic Structure of a Micelle in Solution Determined by Wide Q -Range Neutron Diffraction". *J. Am. Chem. Soc.* 133.41 (2011), pp. 16524–16536. DOI: 10.1021/ja205804k.

Hassan, P. A., G. Fritz, and E. W. Kaler. "Small Angle Neutron Scattering Study of Sodium Dodecyl Sulfate Micellar Growth Driven by Addition of a Hydrotropic Salt". *J. Colloid Interface Sci.* 257.1 (2003), pp. 154–162. DOI: 10.1016/S0021-9797(02)00020-6.

Hayward, D. W., J. B. Gilroy, P. A. Rupar, L. Chabanne, C. Pizzey, M. A. Winnik, G. R. Whittell, I. Manners, and R. M. Richardson. "Liquid Crystalline Phase Behavior of Well-Defined Cylindrical Block Copolymer Micelles Using Synchrotron Small-Angle X-Ray Scattering". *Macromolecules* 48.5 (2015), pp. 1579–1591. DOI: 10.1021/ma502222f.

Hazell, G., A. P. Gee, T. Arnold, K. J. Edler, and S. E. Lewis. "Langmuir Monolayers Composed of Single and Double Tail Sulfobetaine Lipids". *J. Colloid Interface Sci.* 474 (2016), pp. 190–198. DOI: 10.1016/j.jcis.2016.04.020.

Humphrey, W., A. Dalke, and K. Schulten. "VMD: Visual Molecular Dynamics". *J. Mol. Graph.* 14.1 (1996), pp. 33–38. DOI: 10.1016/0263-7855(96)00018-5.

ILL: Neutron for Science: Technical Characteristics. URL: https://www.ill.eu/reactor-environment-safety/high-flux-reactor/technical-characteristics/ (Accessed 2016-8-8).

ISIS – How ISIS Works. URL: https://www.isis.stfc.ac.uk/Pages/What-does-ISIS-Neutron-Muon-Source-do.aspx (Accessed 2018-9-25).

Israelachvili, J. *Intermolecular and Surface Forces*. 3rd ed. Cambridge, USA: Academic Press, 2011. ISBN: 978-0-12-391933-5.

Ivanović, M. T., L. K. Bruetzel, J. Lipfert, and J. S. Hub. "Temperature-Dependent Atomic Models of Detergent Micelles Refined against Small-Angle X-Ray Scattering Data". *Angew. Chemie Int. Ed.* 57.20 (2018), pp. 5635–5639. DOI: 10.1002/anie.201713303.

Jensen, G. V., R. Lund, J. Gummel, T. Narayanan, and J. S. Pedersen. "Monitoring the Transition from Spherical to Polymer-like Surfactant Micelles Using Small-Angle X-Ray Scattering". *Angew. Chemie Int. Ed.* 53.43 (2014), pp. 11524–11528. DOI: 10.1002/anie.201406489.

Jones, R. A. L. *Soft Condensed Matter*. Oxford, UK: Oxford University Press, 2002. ISBN: 978-0-19-850589-1.

Jurašin, D., M. Vinceković, A. Pustak, I. Šmit, M. Bujan, and N. Filipović-Vinceković. "Lamellar to Hexagonal Columnar Liquid Crystalline Phase Transition in a Catanionic Surfactant Mixture: Dodecylammonium Chloride–Sodium Bis(2-Ethylhexyl) Sulfosuccinate". *Soft Matter* 9.12 (2013), p. 3349. DOI: 10.1039/c3sm27665a.

Kataoka, K., A. Harada, and Y. Nagasaki. "Block Copolymer Micelles for Drug Delivery: Design, Characterization and Biological Significance". *Adv. Drug Deliv. Rev.* 64 (2012), pp. 37–48. DOI: 10.1016/j.addr.2012.09.013.

Kennedy, J. and R. Eberhart. "Particle Swarm Optimization". In: *Proceedings of ICNN'95*. International Conference on Neural Networks. Perth, AU: IEEE, 1995, pp. 1942–1948. DOI: 10.1109/ICNN.1995.488968.

Kewalramani, S., H. Hlaing, B. M. Ocko, I. Kuzmenko, and M. Fukuto. "Effects of Divalent Cations on Phase Behavior and Structure of a Zwitterionic Phospholipid (DMPC) Monolayer at the Air–Water Interface". *J. Phys. Chem. Lett.* 1.2 (2010), pp. 489–495. DOI: 10.1021/jz9002873.

Kmiecik, S., D. Gront, M. Kolinski, L. Wieteska, A. E. Dawid, and A. Kolinski. "Coarse-Grained Protein Models and Their Applications". *Chem. Rev.* 116.14 (2016), pp. 7898–7936. DOI: 10.1021/acs.chemrev.6b00163.

Koutsioubas, A. "Combined Coarse-Grained Molecular Dynamics and Neutron Reflectivity Characterization of Supported Lipid Membranes". *J. Phys. Chem. B* 120.44 (2016), pp. 11474–11483. DOI: 10.1021/acs.jpcb.6b05433.

Kraft, D. J., J. Hilhorst, M. A. P. Heinen, M. J. Hoogenraad, B. Luigjes, and W. K. Kegel. "Patchy Polymer Colloids with Tunable Anisotropy Dimensions". *J. Phys. Chem. B* 115.22 (2011), pp. 7175–7181. DOI: 10.1021/jp108760g.

Kratky, O and G Porod. "Diffuse Small-Angle Scattering of x-Rays in Colloid Systems". *J. Colloid Sci.* 4.1 (1949), pp. 35–70. DOI: 10.1016/0095-8522(49)90032-X.

Lu, J. R., E. M. Lee, and R. K. Thomas. "The Analysis and Interpretation of Neutron and X-Ray Specular Reflection". *Acta Crystallogr. A* 52.1 (1996), pp. 11–41. DOI: 10.1107/S0108767395011202.

Marrink, S. J., H. J. Risselada, S. Yefimov, D. P. Tieleman, and A. H. de Vries. "The MARTINI Force Field: Coarse Grained Model for Biomolecular Simulations". *J. Phys. Chem. B* 111.27 (2007), pp. 7812–7824. DOI: 10.1021/jp071097f.

McCluskey, A. R. and K. J. Edler. "Model-Dependent Small-Angle Scattering for the Study of Complex Organic Materials". *Curr. Org. Chem.* 22.8 (2018), pp. 750–757. DOI: 10.2174/1875692115666170612104439.

McCluskey, A. R., J. Grant, A. J. Smith, J. L. Rawle, D. J. Barlow, M. J. Lawrence, S. C. Parker, and K. J. Edler. "Assessing Molecular Simulation for the Analysis of Lipid Monolayer Reflectom-

etry". *J. Phys. Comm.* Accepted (2019). DOI: 10.1088/2399-6528/ab12a9.

McCluskey, A. R., J. Grant, A. R. Symington, T. Snow, J. Doutch, B. J. Morgan, S. C. Parker, and K. J. Edler. "An Introduction to Classical Molecular Dynamics Simulation for Experimental Scattering Users". *J. Appl. Crystallogr.* Accepted (2019).

McCluskey, A. R., B. J. Morgan, K. J. Edler, and S. C. Parker. "Pylj: A Teaching Tool for Classical Atomistic Simulation". *J. Open Source Educ.* 1.2 (2018), pp. 19–21. DOI: 10.21105/jose.00019.

McCluskey, A. R., A. Sanchez-Fernandez, K. J. Edler, S. C. Parker, A. J. Jackson, R. A. Campbell, and T. Arnold. "Bayesian Determination of the Effect of a Deep Eutectic Solvent on the Structure of Lipid Monolayers". *Phys. Chem. Chem. Phys.* 21.11 (2019), pp. 6133–6141. DOI: 10.1039/C9CP00203K.

MetalJet X-Ray Source Technology. URL: https://www.excillum.com/technology/ (Accessed 2018-12-6).

Miller, A. F., M. R. Wilson, M. J. Cook, and R. W. Richards. "Monte Carlo Simulations of an Amphiphilic Polymer at a Hydrophobic/Hydrophilic Interface". *Mol. Phys.* 101.8 (2003), pp. 1131–1138. DOI: 10.1080/0026897031000068569.

Mohwald, H. "Phospholipid and Phospholipid-Protein Monolayers at the Air-Water Interface". *Annu. Rev. Phys. Chem.* 41 (1990), pp. 441–476. DOI: 10.1146/annurev.pc.41.100190.002301.

Nelson, A. R. J. and S. W. Prescott. "Refnx: Neutron and X-Ray Reflectometry Analysis in Python". *J. Appl. Crystallogr.* 52.1 (2019), pp. 193–200. DOI: 10.1107/S1600576718017296.

Pambou, E., J. Crewe, M. Yaseen, F. N. Padia, S. Rogers, D. Wang, H. Xu, and J. R. Lu. "Structural Features of Micelles of Zwitterionic Dodecyl-Phosphocholine (C_{12} PC) Surfactants Studied by Small-Angle Neutron Scattering". *Langmuir* 31.36 (2015), pp. 9781–9789. DOI: 10.1021/acs.langmuir.5b02077.

Pedersen, J. S. "Monte Carlo Simulation Techniques Applied in the Analysis of Small-Angle Scattering Data from Colloids and Polymer System". In: *Neutron, X-Rays and Light. Scattering Methods Applied to Soft Condensed Matter*. Ed. by Th. Zemb and P. Lindner. Amsterdam, NL: Elsevier Science B.V., 2002, pp. 381–390. ISBN: 978-0-08-093013-8.

Rodriguez-Loureiro, I., E. Scoppola, L. Bertinetti, A. Barbetta, G. Fragneto, and E. Schneck. "Neutron Reflectometry Yields Distance-Dependent Structures of Nanometric Polymer Brushes Interacting across Water". *Soft Matter* 13.34 (2017), pp. 5767–5777. DOI: 10.1039/C7SM01066D.

Rondelli, V., G. Fragneto, S S., E. Del Favero, and L. Cantù. "Reflectivity from Floating Bilayers: Can We Keep the Structural Asymmetry?" *J. Phys. Conf. Ser.* 340 (2012), p. 012083. DOI: 10.1088/1742-6596/340/1/012083.

Rose, D. R., J. Phipps, J. Michniewicz, G. I. Birnbaum, F. R. Ahmed, A. Muir, W. F. Anderson, and S. Narang. "Crystal Structure of T4-Lysozyme Generated from Synthetic Coding DNA Expressed in Escherichia Coli". *Protein Eng. Des. Sel.* 2.4 (1988), pp. 277–282. DOI: 10.1093/protein/2.4.277.

Rosen, M. J. and J. T. Kunjappu. *Surfactants and Interfacial Phenomena*. 4th ed. Hoboken, USA: John Wiley & Sons, 2012. ISBN: 978-0-470-54194-4.

Sammalkorpi, M., M. Karttunen, and M. Haataja. "Ionic Surfactant Aggregates in Saline Solutions: Sodium Dodecyl Sulfate (SDS) in the Presence of Excess Sodium Chloride (NaCl) or Calcium Chloride ($CaCl_2$)". *J. Phys. Chem. B* 113.17 (2009), pp. 5863–5870. DOI: 10.1021/jp901228v.

Schmaljohann, D. "Thermo- and pH-Responsive Polymers in Drug Delivery". *Adv. Drug Deliv. Rev.* 58.15 (2006), pp. 1655–1670. DOI: 10.1016/j.addr.2006.09.020.

Schnablegger, H. and Y. Singh. *The SAXS Guide: Getting Acquainted with the Principles*. 4th ed. Graz, AT: Anton Paar GmbH, 2017.

Schramm, L. L., E. N. Stasiuk, and D. G. Marangoni. "Surfactants and Their Applications". *Annu. Rep. Prog. Chem., Sect. C: Phys. Chem.* 99 (2003), pp. 3–48. DOI: 10.1039/B208499F.

Scoppola, E. and E. Schneck. "Combining Scattering and Computer Simulation for the Study of Biomolecular Soft Interfaces". *Curr. Opin. Colloid Interface Sci.* 37 (2018), pp. 88–100. DOI: 10.1016/j.cocis.2018.06.008.

Shi, Y. and R. Eberhart. "A Modified Particle Swarm Optimizer". In: *1998 IEEE International Conference on Evolutionary Computation Proceedings*. IEEE World Congress on Computational Intelligence. Anchorage, US: IEEE, 1998, pp. 69–73. DOI: 10.1109/ICEC.1998.699146.

Simons, K. and D. Toomre. "Lipid Rafts and Signal Transduction". *Nat. Rev. Mol. Cell Biol.* 1 (2000), pp. 31–39. DOI: 10.1038/35036052.

Sivia, D. S. *Elementary Scattering Theory: For X-Ray and Neutron Users*. Oxford, UK: Oxford University Press, 2011. ISBN: 978-0-19-922868-3.

Storn, R. and K. Price. "Differential Evolution – A Simple and Efficient Heuristic for Global Optimization over Continuous Spaces". *J. Global Optim.* 11 (1997), pp. 341–359. DOI: 10.1023/A:1008202821328.

Wormington, M., C. Panaccione, K. M. Matney, and D. K. Bowen. "Characterization of Structures from X-Ray Scattering Data Using Genetic Algorithms". *Philos. Trans. R. Soc. London Ser. A* 357.1761 (1999), pp. 2827–2848. DOI: 10.1098/rsta.1999.0469.

Zagnoni, M. "Miniaturised Technologies for the Development of Artificial Lipid Bilayer Systems". *Lab on a Chip* 12.6 (2012), p. 1026. DOI: 10.1039/c2lc20991h.